

## Non-condensable Gas Effect During a Late Reflood Phase of the LBLOCA

Yusun Park<sup>a\*</sup>, Hyun-sik Park<sup>a</sup>, Kyoung-ho Kang<sup>a</sup>, Nam-hyun Choi<sup>a</sup>,  
Kyoung-ho Min<sup>a</sup>, Ki-yong Choi<sup>a</sup>

<sup>a</sup>Thermal Hydraulics Safety Research Division, Korea Atomic Energy Research Institute  
989-111 Daedeok-daero, Yuseong-gu, Daejeon, 305-333, Republic of Korea

\*Corresponding author: yusunpark@kaeri.re.kr

### 1. Introduction

During normal operation of the nuclear power plant, the upper part of the SITs is filled with nitrogen gas, which is pressurized at around 4.3 MPa. In the case of the LBLOCA, when the primary pressure becomes lower than the nitrogen pressure, the nitrogen gas can flow into the reactor coolant system after termination of the SIT injection. It can be expected that the nitrogen gas injection has a positive effect from the view point of the core cooling performance. However, there are currently no available experimental data to confirm this expectation.

Thus, an experimental study of the nitrogen gas effect during the reflow phase of an LBLOCA was conducted to evaluate the core cooling performance of the 4 trains ECCS with an assumption of a single failure. The overall experimental results were analyzed to confirm that the thermal hydraulic phenomenon of the late reflow phase was successfully simulated. In addition to that, the test result was evaluated against the other experimental case in which the nitrogen gas was not injected to show the effect of the nitrogen gas, especially in the view point of the core quenching time.

### 2. Description of the ATLAS

#### 2.1 General description of the ATLAS

The ATLAS facility includes a reactor pressure vessel, two steam generators, four reactor coolant pumps, a pressurizer, and four safety injection tanks. The detailed ATLAS design and description of the ATLAS development program can be found in the literature [1, 2]. Arrangement and labeling of the primary legs including the break simulation lines are also shown together. The number of instruments is up to 1,300 at present, and the detailed description of the signal processing system and control system of the ATLAS can be found in the literature [3, 4].

#### 2.2 Break simulation system for the LBLOCA test

The configuration of the break simulation system and containment simulation system used for the LBLOCA reflow tests were described in detail in the literature [5].

The break simulation system consists of a quick opening valve, located on the clod leg, a break nozzle, a case holding the break nozzle, and a few instruments. The break area is scaled down to match the pressure drop through the break line. The break flow is discharged into a containment simulation system, which consists of separating vessels and measuring vessels. The ATLAS has two separating vessels. In the case of the double-ended guillotine LBLOCA, both separating vessels are designed to be used simultaneously. The separating vessel is also designed to simulate a containment back-pressure by controlling its pressure using a pressure control valve.

#### 2.3. Non-condensable gas injection system

In this test, the nitrogen gas was injected into the primary system after the SIT injection was terminated. When the SITs have specified levels of 85% at the initial state, the pressure of the nitrogen gas, which was filled in the upper part of the SIT, was around 2.4 MPa. With the continuous injection of the ECC water from SITs, the pressure of the nitrogen gas was decreased and reached around 0.7 MPa when the SIT injection was terminated. After the SIT injection was stopped, the nitrogen gas flowed into the primary system through the stand pipes which was installed in the SIT until the pressure of the nitrogen gas of the upper part of the SIT became the same with that of the primary system

### 3. Experimental Conditions and Procedure

Before the test, a heat-up of the whole system and an initialization process was carried out to obtain the steady state of the whole system. The overall procedures to achieve the initial steady state are explained in the literature [6]. About 10 minutes after the steady-state conditions were achieved, both in the primary and secondary system, the water inventory in the reactor pressure vessel was discharged using the four FCV valves (FCV-DVI-01~04), which were newly installed valves on the DVI lines.

The sequence of events of the LBLOCA test (Test ID: LB-SI-05) is summarized in Table 1. The decay heat was simulated from the start time for the reflow phase of a LBLOCA along the ANS-73 decay curve. The scaled ECC water flow rates from the four safety

injection tanks and three high pressure safety injection pumps were injected as the designed flow rates.

The nitrogen gas was injected to the primary system through the stand pipes which were installed in the SITs after the SIT injection was terminated. The amount of the nitrogen gas injected to the primary system was estimated using the ideal gas equation. The amount of the injected nitrogen gas was a little different for each tank and the total amount from the four SITs was calculated as 5.18 kg.

Table 1: Sequence of Event

Event	Time (DAS)	Description
Test Start	0	Data recording start
Heating End	302	Core/RCP Trip, SS Isolation, Heater off
Vent/Drain	325~1104	FCV-DVI-01~04 Open
BS Open	1116	FCV-BS-02, OV-BS-01 Open
IL Drain	Manual	Intermediate lines are emptied.
Power Restart	1216	Linear increase during 20 seconds
SIT Injection	1271	Max T>450 °C
Reflow Start	1273	2.0 s after SIT Injection
SIP Injection	1286	12.7 s after Reflood start
PCT	1373	Peak Heater rod surface temperature, 633.82 °C
Quenching	1588	TH-CO-G2-MAX

#### 4. Results

Fig. 1 presents a core power variation during the test. The core power was restarted at 1,216 seconds. In the beginning the core power increased linearly within 20 seconds to 1,186 Kw. It was remained constant until it intersected with the scaled decay power at which the reflow starts then, controlled to decay down following a scaled power of 1.2 times that of the ANS-73 decay curve.

Fig. 2 presents the variation of the primary system pressures during the test. The primary system pressure was maintained at atmospheric pressure until the ECC water was injected. When the ECC water began to be injected, the primary system pressure started to increase rapidly. After the primary pressure reached a peak pressure of 0.28 MPa, it decreased gradually.

Fig. 3 presents the wide-range water level variations in both the core and downcomer regions. On initiating the reflow, the water levels in both the core and downcomer regions increased rapidly. However, they decreased with a decreased ECC flow rate and a spillover of the water inventory. The water levels were then decreased by the entrainment or off-take of the droplets, possibly generated by a downcomer boiling in

the downcomer region. After this, the water levels steadily increased owing to the lowered wall temperature in the downcomer and a sufficient cooling capacity of the ECC water injected by the SIP.

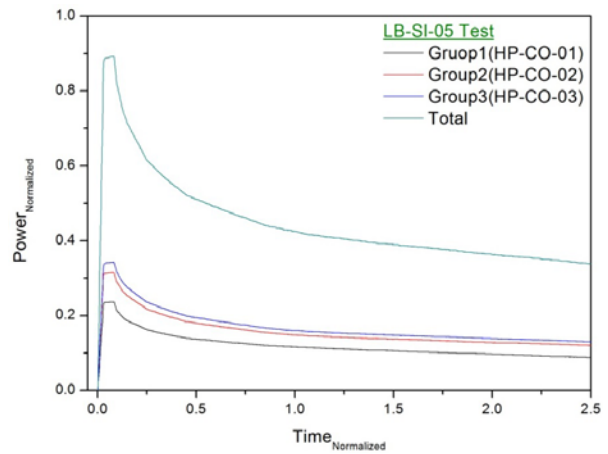


Fig. 1 Core Power Variations

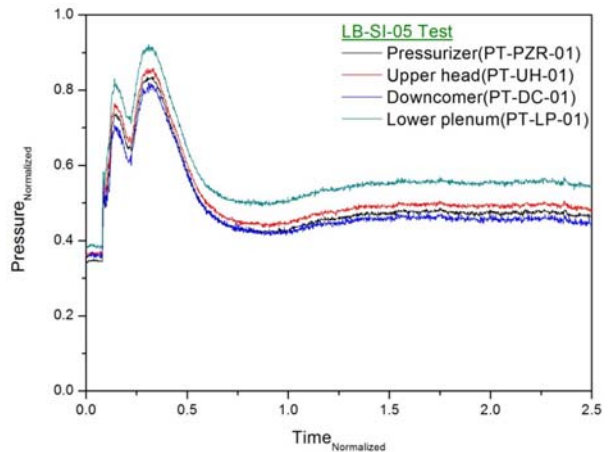


Fig. 2 Primary System Pressure Variations

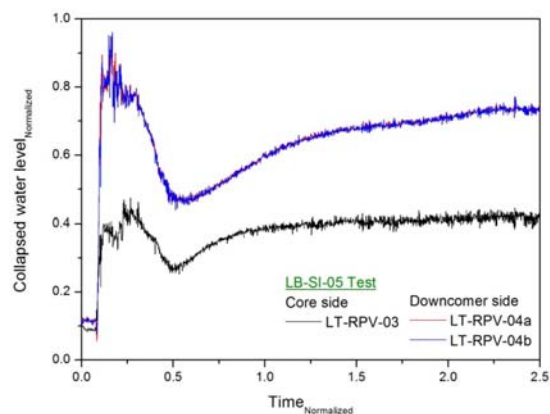


Fig. 3 Wide Range Water Level Variations of the RPV

Fig. 4 presents the maximum surface temperature variations of the core heater rods during the test. The maximum surface temperature of the heater rod was 633.82 °C. The entire rewetting process was finished by about 315 seconds after the reflow start time.

Fig. 5 presents the variation of the ECC flow rate during the reflood period. It is shown that the required flow rates were successfully provided by the SITs and the three SIPs. The flow rates were slightly different from each other owing to the different system characteristics for the injection lines. Among them, the flow rates from SIT3 showed an abnormal trend. It was supposed a certain error which comes from the instrumentation signal. However, the amount of ECC water injected from SIT3 is confirmed by the amount of level and pressure decrease of SIT3.

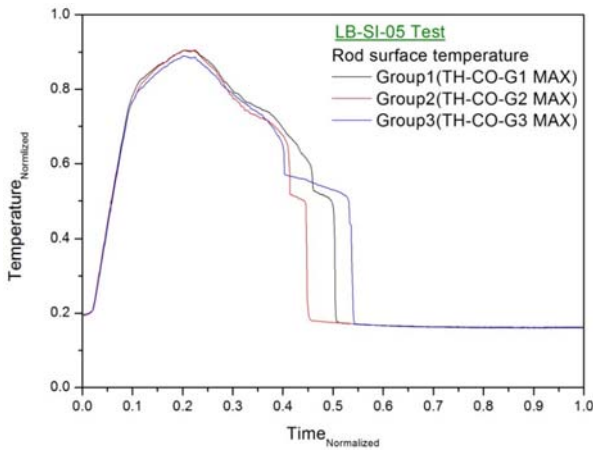


Fig. 4 Maximum Heater Rod Surface Temperature Variations

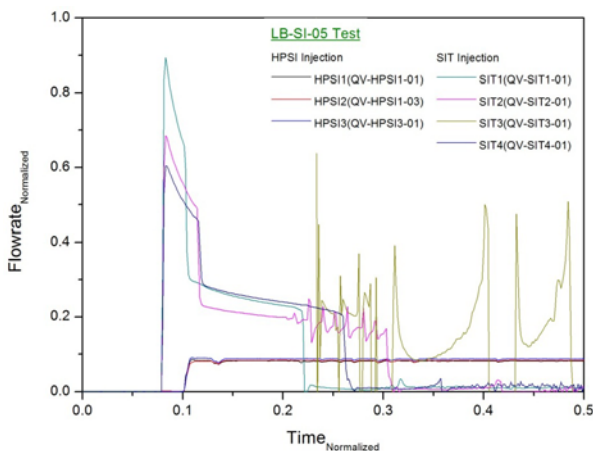


Fig.5 Measured ECC Flow Rate

Fig. 6 and 7 present the variation of water levels and the pressures in the SITs, respectively. Initially the SITs were filled with nitrogen gas at 4.3 MPa. As the water in the SIT was injected to the core, the pressure of the SITs showed an exponential decrease. The decreasing rate was changed to a lower value when the SIT flow was converted into a low flow region. After the termination of the SITs, the water levels in the SITs were not decreased anymore as shown in Fig. 6.

When the ECC water injection from the SITs was terminated, the pressure of the upper part of the SITs, which was filled with the nitrogen gas was about 0.7 MPa. At this time, the pressure of the primary system was around 0.2 MPa. Thus, the nitrogen gas flowed into

the primary system until the pressure of the SITs reached the same pressure of the primary system as shown in Fig 7.

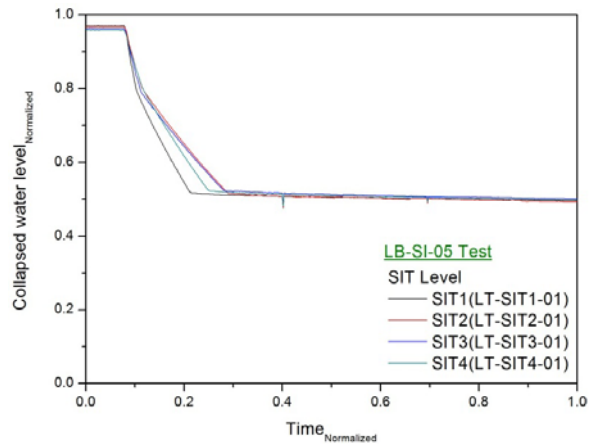


Fig. 6 Water Level Variations in the SIT

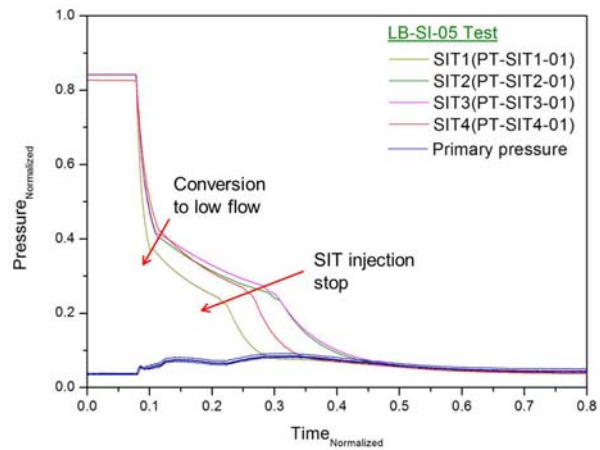


Fig. 7 Pressure Variation of the System with the Nitrogen Gas Injection

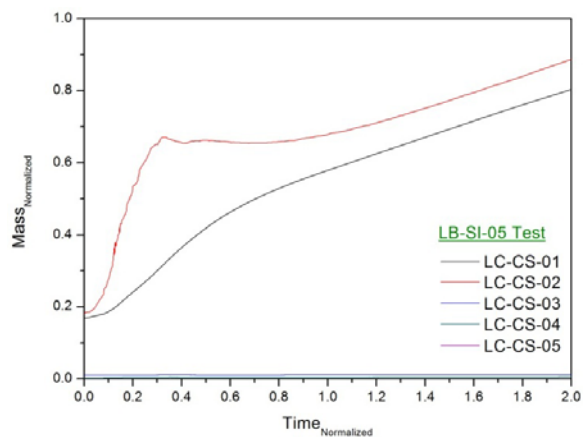


Fig. 8 Water Masses Measured from 5 Measuring Vessels

The variations of the water masses measured from the 5 measuring vessels are presented in Fig. 8. The water masses measured using LC-CS-01~LC-CS-05 were 964.51 kg initially at the reflood start time and they increased owing to the inflow from the break. The

total break flow rate was calculated by a summation of the water and steam flow rates.

Fig 9 shows the water levels comparison in the core and downcomer regions between two test cases. One is the test case (LB-SI-05) in which nitrogen gas was injected and the other one is the test (LB-SI-01R) which was conducted without nitrogen gas injection.

Around 200 seconds after the power restart, the SITs injection was terminated and the water levels started to decrease until the heater rods were quenched. During this period, the water levels in the RPV of the LB-SI-05 test were kept higher than those of the LB-SI-01R case. It can be explained that the injected nitrogen gas pushed down the downcomer water so that the collapsed water level in the core was kept higher.

The higher core water level caused a faster rewetting process on the heater rod. Thus, the quenching of the heater rod surface occurred faster in a shorter time than the LB-SI-01R case, as shown in Fig 10. From the power restart to the quenching, it took 372 seconds in the LB-SI-05 test and 447 seconds in the LB-SI-01R cases, respectively.

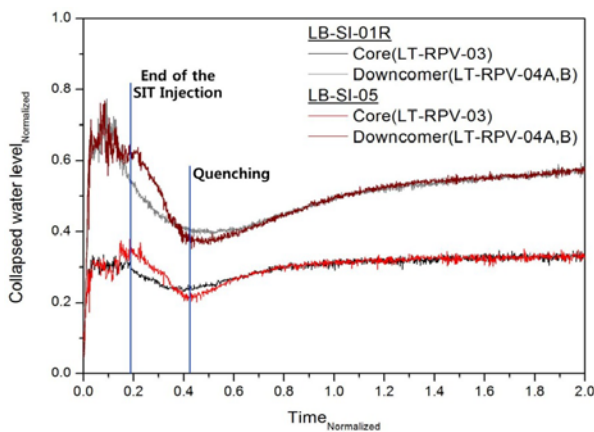


Fig. 9 Comparison of the Primary Water Level

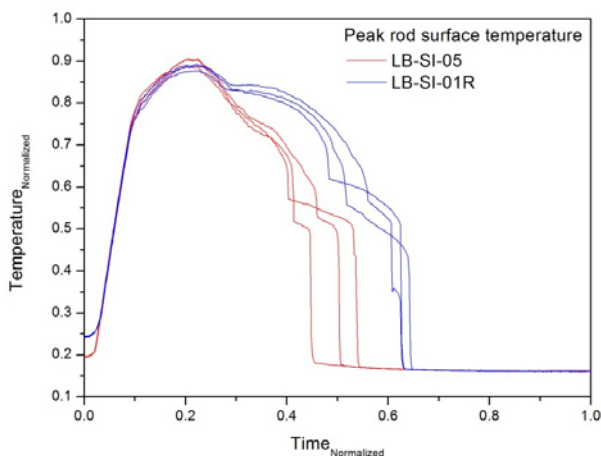


Fig. 10 Comparison of the Peak Cladding Temperatures

An experimental study of the nitrogen gas effect during the reflood phase of an LBLOCA was conducted to evaluate the core cooling performance of the 4 trains ECCS with an assumption of a single failure.

To achieve the initial and boundary conditions of the LBLOCA test at the start of the reflood phase, the primary system was depressurized and drained. The decay heat was simulated from the start time for the reflood phase of a LBLOCA along the ANS-73 decay curve and the scaled ECC water flow rates from the four safety injection tanks and three high pressure safety injection pumps were injected as the designed flow rates. The nitrogen gas was also injected successfully after the termination of four SITs injection.

The overall experimental results revealed the typical thermal-hydraulic trends expected to occur during the reflood phase of a large-break LOCA scenario for the APR1400. The nitrogen gas injected into the system affected the higher water level (20~25%) in the RPV and the shorter quenching time (372 seconds) than those of the other cases which were performed without nitrogen gas injection. Thus, we can conclude that nitrogen gas injection into the RPV has a positive effect from the view point of safety.

## REFERENCES

- [1] H.S. Park., D.J. Euh., K.T. Choi., et al., "Calculation Sheet for the Basic Design of the ATLAS Fluid System," KAERI/TR-3333/2007 (2007).
- [2] K. H. Kang et al., "Detailed Description Report of ATLAS Facility and Instrumentation," KAERI/TR-4316/2011 (2011)
- [3] S. Cho et al., "Description of the Signal Processing System of ATLAS Facility," KAERI/TR-3334/2007 (2007)
- [4] K.Y. Choi et al., "Control and Data Acquisition System of the ATLAS Facility," KAERI/TR-3338/2007 (2007)
- [5] K. H. Kang et al., "Detailed Description Report of Configuration of the ATLAS for LBLOCA Tests," KAERI/TR-4780/2012 (2012)
- [6] K. H. Kang et al., "Standard Test Procedure for ATLAS Integral Effect Test", ATLAS-TP-13-01 (2013)

## 5. Conclusion